Reprinted from
Journal of Imaging Science and Technology® 65(5): 050401-1–050401-13, 2021.

Preliminary Result on the Direct Assessment of Perceptible Simultaneous Luminance Dynamic Range

Fu Jiang▲ **and Mark D. Fairchild**▲
Munsell Color Science Laboratory, Rochester Institute of Technology, Rochester, New York, USA
E-mail: fj4136@rit.edu

Abstract. *The human visual system is capable of adapting across a very wide dynamic range of luminance levels; values up to 14 log units have been reported. However, when the bright and dark areas of a scene are presented simultaneously to an observer, the bright stimulus produces significant glare in the visual system and prevents full adaptation to the dark areas, impairing the visual capability to discriminate details in the dark areas and limiting simultaneous dynamic range. Therefore, this simultaneous dynamic range will be much smaller, due to such impairment, than the successive dynamic range measurement across various levels of steady-state adaptation. Previous indirect derivations of simultaneous dynamic range have suggested between 2 and 3.5 log units. Most recently, Kunkel and Reinhard reported a value of 3.7 log units as an estimation of simultaneous dynamic range, but it was not measured directly. In this study, simultaneous dynamic range was measured directly through a psychophysical experiment. It was found that the simultaneous dynamic range is a bright-stimulus-luminance dependent value. A maximum simultaneous dynamic range was found to be approximately 3.3 log units. Based on the experimental data, a descriptive log-linear model and a nonlinear model were proposed to predict the simultaneous dynamic range as a function of stimulus size with bright-stimulus luminance-level dependent parameters. Furthermore, the effect of spatial frequency in the adapting pattern on the simultaneous dynamic range was explored. A log parabola function, representing a traditional Contrast Sensitivity Function (CSF), fitted the simultaneous dynamic range data well.* © *2021 Society for Imaging Science and Technology.*
[DOI: 10.2352/J.ImagingSci.Technol.2021.65.5.050401]

1. INTRODUCTION

High dynamic range (HDR) displays have gained popularity in recent years for their better capability of color/luminance reproduction, hence improved visual experience. HDR display development started with the traditional prototype that replaced the uniform LCD backlight with a spatially modulated projector [1], evolving to the recent local dimming LCD HDR [2] and OLED HDR display technologies, especially with some advanced material development. The LCD-based display has its advantage of achieving a high peak luminance but is limited in the achievable black level, mainly due to internal reflection and limited minimum transmittance. While OLED displays have the advantage of very pure black, approaching a luminance of 0 cd/m^2 they have some physical limitations of the peak luminance level. Along with the development of the commercial HDR displays, some questions have appeared, e.g. how much dynamic range is enough as for a display [3], how black would be good enough, and what is the impact of the ambient lighting on the HDR display [4]. There is another question remaining: what is the simultaneous dynamic range when the bright and dark stimuli are presented simultaneously. The answer would be of great benefit in some fine-tuning of the high dynamic range imagery, which restricts the adaptation, as well as in devices and algorithms for image capture, processing, and display.

Human visual system has the capability of adapting to about 14 log units of luminance level. From 10^{-6} to 10 cd/m^2 is called scotopic range, where the light transduction is mediated by rods, and from 0.01 to 10^8 cd/m^2 is called photopic range, where the cones are active [5]. The overlapping range is referred to as mesopic vision, where both rods and cones are active. However, it requires a long time, i.e. at least 10–20 min, for human observers to adapt to very low luminance levels. Therefore, in most practical usage, the cones are more significant, which still represents a quite large dynamic range compared with most displays.

Two mechanisms contribute to such a large dynamic range of human luminance sensitivity: adaptation of the cone sensitivity according to the light luminance level, and the dynamic range of the intrinsic response of the cone cells. Variation in pupil diameter also has a role, though its contribution is relatively small. It is known that the first mechanism contributes mostly to the human visual system's large dynamic range, especially when the average luminance level of the target changes dramatically. The second mechanism, the dynamic range of the photoreceptor cells, can be considered the main determinant of the simultaneous dynamic range although some amount of the rapid local adaptation in the cones does occur. Mainly two reasons limit the simultaneous dynamic range of the cones. Firstly, scattering in the optical media reduces the contrast of the retinal stimulus. Secondly, there are optical and neural response limitations on the photoreceptors and the higher-order visual mechanisms. There are two different ways of measuring simultaneous dynamic range: physiological measurement of the excitation of the photoreceptors and psychophysical measurement of the simultaneous dynamic range from the perspective of how much dynamic range observers can discriminate with a stable adapting level. A range of 2–3.5 log units has been reported as the simultaneous dynamic range

▲ IS&T Members.

Received May 26, 2021; accepted for publication Aug. 29, 2021; published online Sep. 29, 2021. Associate Editor: Samuel Morillas.
1062-3701/2021/65(5)/050401/13/$25.00

via physiological measurement of the excitation of the photoreceptors. Myers reported 2 log units of simultaneous dynamic range [6], Purves and Lotto presented a value of 3 log units [7], and Norman showed a stable value of 3.5 log units regardless of the background [8]. There is quite a large discrepancy, largely due to the measurement technology and the lack of clear definition of simultaneous dynamic range.

Simultaneous dynamic range, as indicated by its name, should be defined as the dynamic range when observers can discriminate some details in the bright area and dark area at the same time or within a limited observing time. The most recent study of assessment of the simultaneous dynamic range was reported by Kunkel and Reinhard, who used a psychophysical methodology [9]. Kunkel and Reinhard measured the observers' ability to discriminate a certain contrast level above and below the adapting level separately. Those were considered as the upper and lower bounds of the cone response curve at a certain adapting level. The ratio between the upper and lower bounds was considered as the simultaneous dynamic range. They reported a maximum of 3.7 log units of simultaneous dynamic range, which is the higher than most previous studies. There are two reasons why they found a higher value: (1) separate measurement of the upper and lower bounds allows the shifting of the adapting level, which would overestimate both bounds in some degree; and (2) the separate measurement of the upper and lower bounds underestimates the effect of the glare on the lower bound, mainly caused by the upper bound. Therefore, 3.7 log units is expected to be an overestimated value compared with direct measurement of the simultaneous dynamic range.

In this study, to address the limitations of the Kunkel and Reinhard study, simultaneous dynamic range was measured directly with a bright-dark spatially-alternating pattern. The bright-dark spatially-alternating pattern used is unique to this study. The pattern introduces bright and dark regions at the same time. Theoretically, the discriminating detail ability on both the bright and the dark regions should be measured. However, it is known that observers will always be able to discriminate some details in the bright region as long as the details reach a threshold. Such a threshold usually is measured as a contrast sensitivity function, which is well generalized by Barten's model [10]. Therefore, it is more important to explore the impairment of human ability in perceiving the contrast in dark region from the bright region. In this study, a 5% contrast Gabor pattern on the dark region was used as the criterion for defining simultaneous dynamic range. Observers' ability in discriminating such a pattern in the dark region was measured. The effect of the bright stimulus luminance level and the effect of the stimulus size were explored as well. The experimental data were used to build a mathematical model to describe the simultaneous dynamic range results. Furthermore, the impact of spatial frequency of the contrast pattern was explored.

2. EXPERIMENTAL SETUP

As stated in the introduction, the goal is measuring the simultaneous dynamic range of the human visual system while viewing typical image displays. Due to the well explored and modeled contrast sensitivity function in the bright region, it is more important to explore observers' ability to discriminate contrast in dark regions when adjacent to bright regions. In this study, a 5% contrast Gabor pattern was used as the discriminating criterion. The 5% is set as an initial contrast level for simultaneous dynamic range study and based on hardware limitations. It should be noted that lower contrast levels as the criterion would result in reduced estimates of dynamic range and 5% can be considered a reasonable threshold for perceiving image details in the shadow regions.

2.1 *Experiment Design*

The experimental image was designed to contain both bright and dark stimulus areas. In measuring simultaneous dynamic range, an edge-blurred Gabor pattern in the dark stimulus was used as the discrimination criterion. The edge-blurred Gabor pattern was designed according to Eq. (1), where L_0 is the mean luminance level, C controls the contrast level of the Gabor pattern, x is the horizontal location, $x0$ is the horizontal location of the center of the stimulus, t is the horizontal length of one full cycle, and S is a edge-smoothing function shown in Eq. (2), a rectangular function multiplying with a high order ($n = 5$) cosine function. The rectangular function is a cut-off function with a diameter of $2 \times r0$, and $(x0, y0)$ is the central position of the Gabor pattern. Equation (1) would create a Gabor pattern with a certain Michelson contrast level. Michelson contrast is defined as $((I_{\max} - I_{\min})/(I_{\max} + I_{\min}))$, which is equal to $(2 * C)/(2 * L_0) = C/L_0$ based on Eq. (1). Equation (1) can also be used to create an edge-smoothing uniform area by setting the C to 0.

$$Y(x, y) = \left(L_0 + C \times \cos\left(2\pi \times \frac{x - x0}{t}\right)\right) \times S \tag{1}$$

$$S = \text{rect}\left(\frac{r}{2 \times r0}\right) \times 0.5 \times \left(1 + \left(\cos\left(\frac{r}{r0} \times \pi\right)\right)^n\right)$$
$$r = ((x - x0)^2 + (y - y0)^2)^{1/2}. \tag{2}$$

In this experiment, a 2AFC (two alternative forced choice) procedure was adopted. The observers were asked to find the Gabor pattern within the experimental image across two possible locations. Six to eight different levels of Gabor pattern images were used for each threshold measurement. Figure 1 shows two examples of the experimental image. Both are bright-dark alternating images with a flip of the bright and dark positions. Inside the gray box, there are two identical bright stimuli and two dark stimuli with the same mean luminance level. One of the dark stimuli (top right in the left example, top left in the right example) inside the gray box contains a Gabor pattern, and the other dark stimulus is an edge-smoothed uniform area. Outside of the gray box are just bright stimuli with the same luminance levels, the remaining of which was just black (close to 0 cd/m^2). The observer's task was to find the dark stimulus containing

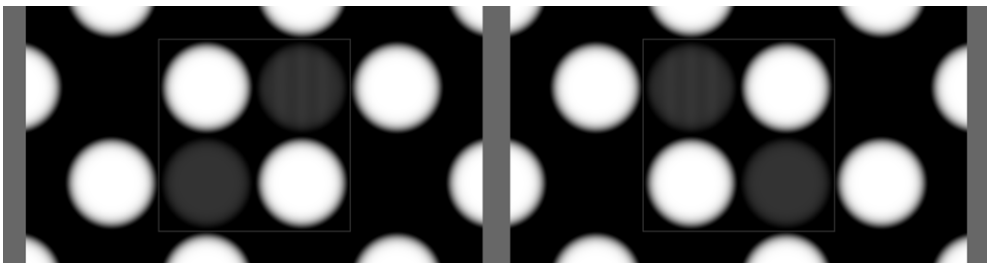

Figure 1. Illustration of experimental image.

the Gabor pattern. The observer could indicate the choice through left-arrow or right-arrow on the keyboard. It should be noted that the variance of the Gabor pattern was kept on horizontal direction during the whole experiment. Moreover, through the whole study, 5% contrast in dark region was set as the constant test level, i.e. 0.1 log unit in dynamic range. Therefore, C in Eq. (1) was set as $5\% \times L_0$, resulting in 5% Michelson contrast Gabor pattern. The examples in Fig. 1 are not actually 5% but have greater contrast to illustrate the experimental image configuration.

2.2 *Apparatus*

An Apple Pro XDR display was used for the experiment. The Apple XDR display is an LCD with a spatially-modulated back-light controlled by 576 individual LED zones [11]. The display is capable of reaching a peak luminance of 1600 cd/m^2 and 1000 cd/m^2 sustained full-screen luminance. The display has a size of 71.8 cm by 41.2 cm with a resolution of 6016 by 3384 pixels. The display was controlled by software developed in Xcode using Objective-C. The software could apply and display 10-bit precision data. The display allows a setting of a diffuse white level, which was set to 50 cd/m^2 and the peak luminance was set to 1600 cd/m^2. Also, in order to reach the 1600 cd/m^2, the experimental image was placed the central $80\% \times 80\%$ area of the panel. The remaining area of the panel was set as 44.28 cd/m^2.

Since this is a LCD display, there is image content depending internal reflection. Especially for the dark level, the internal reflection became significant. This is more severe in our experimental image, where the bright regions alternate with the dark regions. Therefore, there is no standard colorimetric model in characterizing the display while measurements were taken for different settings of the bright stimuli. A CR-100 tristimulus colorimeter was used to measure both the bright stimulus and the dark stimulus. CR-100 was integrated with a large-size sensor for a better precision quick-time in measuring low-luminance stimulus. CR-100 is capable of measuring a range of 0.0007 cd/m^2 to 5140 cd/m^2 with a maximum exposure time of 20 s [12].

The experiment was conducted in a totally dark room with black cloth covering the walls, preventing any possible reflected flare onto the panel. Also two black foam boards were placed on the side of the panel as an additional step to ensure as flare-free environment as possible. The table was covered with black cloth as well. Figure 2 illustrates a top

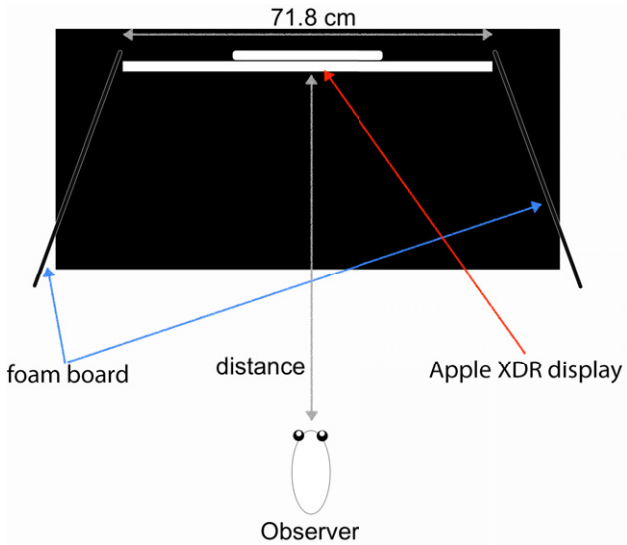

Figure 2. Schematic top view of the experimental setup with the Apple XDR display on the black-cloth covered table along with two black foam boards.

view of the experiment setup. The viewing distance was not constant for the experiment, as described in the following section.

2.3 *Stimuli*

Due to the limitation of the Apple XDR display, as a back-light LCD display, the smaller the stimulus size is, the more internal reflection and leaked light present, resulting in a higher minimal luminance level. Therefore, after some testing, a fixed stimulus size was adopted for the entire experiment. While the experimental image had the configuration shown in Fig. 1, the diameter of the bright and the dark stimulus areas was 118.6 mm, incorporating several backlight zones within each stimulus area.

In this experiment, there were four different luminance levels of the bright regions, as 252 cd/m^2, 452 cd/m^2, 850 cd/m^2 and 1600 cd/m^2. For each bright region luminance setting, the black level was calibrated accordingly to generated Look-Up-Tables (LUTs) between the actual luminance and the input digital count. The LUTs were used to map the desired luminance level to the input digital count, sent to the display. For example, the black level, 0 input digital count, was around 0.0497 cd/m^2, 0.1001 cd/m^2, 0.2393 cd/m^2, 0.2955 cd/m^2 for 252 cd/m^2, 452 cd/m^2,

850 cd/m^2, 1600 cd/m^2 bright stimuli respectively. Again, in this study, 5% contrast in Gabor pattern was set as the discrimination criterion, where C was set as 5% $\times$ L_0 in Eq. (1).

Also, to explore the effect of the stimulus size on the simultaneous dynamic range, four viewing distances, visually equivalent to changing the stimulus size, were tested at 2000 mm, 3000 mm, 4000 mm, 5000 mm. The diameters of the stimulus regions were thus equal to subtended visual angles of 3.4°, 2.27°, 1.7° and 1.36°.

3. EXPERIMENTS AND RESULTS

Two experiments were conducted in this study. The first experiment focused on exploring how the simultaneous dynamic range changes with different luminance levels of the bright regions and different stimulus sizes. The second experiment focused on the impact of the Gabor pattern spatial frequency on simultaneous dynamic range.

3.1 *Experiment I*

3.1.1 *Experimental Images*

For the four different luminance levels of the bright area, L_0 was set as the target luminance level L_{bright}, and C was set as 0 (recall Eq. (1)). For better precision, the method of constant stimulus was used in measuring the simultaneous dynamic range. More details about the method can be found in Engeldrum [13]. For each bright luminance level L_{bright}, there were at least 6 different levels of L_{dark}. Again, C was set as 5% $\times$ L_{dark} for constant 5% contrast. The exact number of dark stimulus luminance levels was determined in a pilot test. Moreover, the luminance levels of these steps vary with the L_{bright}. For each L_{bright} and L_{dark}, both types of bright-dark alternating images, as shown in Fig. 1, were created. In each image, one of the two dark stimuli was randomly selected as the Gabor pattern, and the other dark stimulus was set as constant luminance area. The order of all the experimental images was randomized for each observer.

Additionally, all four different stimulus sizes, i.e. equivalent to viewing distance in this experiment, were measured as well. The luminance level of the bright region L_{bright} was the same for different viewing distances. But the L_{dark} varied with the viewing distance accordingly.

Another important parameter was the spatial frequency of the Gabor pattern. According to the most recent work by Wuerger, Ashfra et al., the human visual system has a maximum contrast sensitivity at around 2 cycles per degree (*cpd*) [14]. Therefore, the primary spatial frequency was set at 2 *cpd* with appropriate t in Eq. (1). But, it is known that the cycle numbers of the sinusoidal pattern also have an impact on the measured human sensitivity [14, 15]. Therefore, a minimum of four cycles of the sinusoidal pattern was also used. Therefore, for the smaller stimulus size, the spatial frequency was slightly higher than 2 *cpd*. The final spatial frequencies of the Gabor pattern were 2 *cpd*, 2 *cpd*, 2.35 *cpd* and 2.94 *cpd* for 2000 mm, 3000 mm, 4000 mm and 5000 mm respectively. The spatial frequency of the Gabor pattern was within 2–5 cpd, the traditional peak sensitivity range [15, 16].

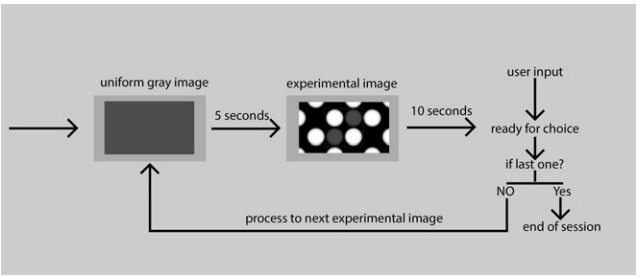

Figure 3. Flowchart of the experiment.

3.1.2 *Procedure*

Figure 3 shows the flow chart of the experiment. The experiment started with one gray image, 1.025 cd/m^2. The usage of this non-minimal uniform image can prevent the observer taking advantage of the after image of the darkest image to detect the Gabor pattern. During the pilot test, it was found that if the image was set as the minimal black, the after image can be used to detect the Gabor pattern. Therefore, a slight above-minimal image was used to prevent this possible "cheating" method. After 5 s, the experimental image was presented with a minimum of 10 s observation time, the system would display a text label indicating that the observer could make a choice. The observers were asked not to spend too much time on each trial, preventing after images. There were 5 s of the dark uniform image before the next experimental image. The order of the experimental images was randomized for each observer.

3.1.3 *Observers*

One observer, OBS1, participated for all the four luminance levels of the bright regions and all four different stimulus sizes. OBS1 made 28 repetitions of all the trials. Another five observers participated for two luminance levels, 452 cd/m^2 and 1600 cd/m^2, of the bright regions with three different stimulus sizes, i.e. viewing distances at 2000 mm, 3000 mm and 4000 mm. All observers were color normal and had corrected, or natural 20/20 visual acuity. None of the observers had difficulty in focusing when viewing distance changes. Ages ranged from 25 to 35 years. The five observers made four repetitions of all conditions, making 20 repetitions of each trial.

3.1.4 *Results*

Result of OBS1. Figure 4 plots the measured threshold of the 5% contrast Gabor pattern on the left and the simultaneous dynamic range on the right. The threshold is defined as the minimum dark stimulus background luminance at which 5% Gabor pattern can be detected on 75% of trails (50% stands for random guess, and 100% for absolution detection). The simultaneous dynamic range can be simply computed as the ratio between the bright stimulus luminance level and the measured threshold dark luminance level, $L_{\text{bright}}/L_{\text{threshold}}$. The horizontal axis in both plots is the stimulus diameter size on a log scale. Each line represents constant bright region luminance level.

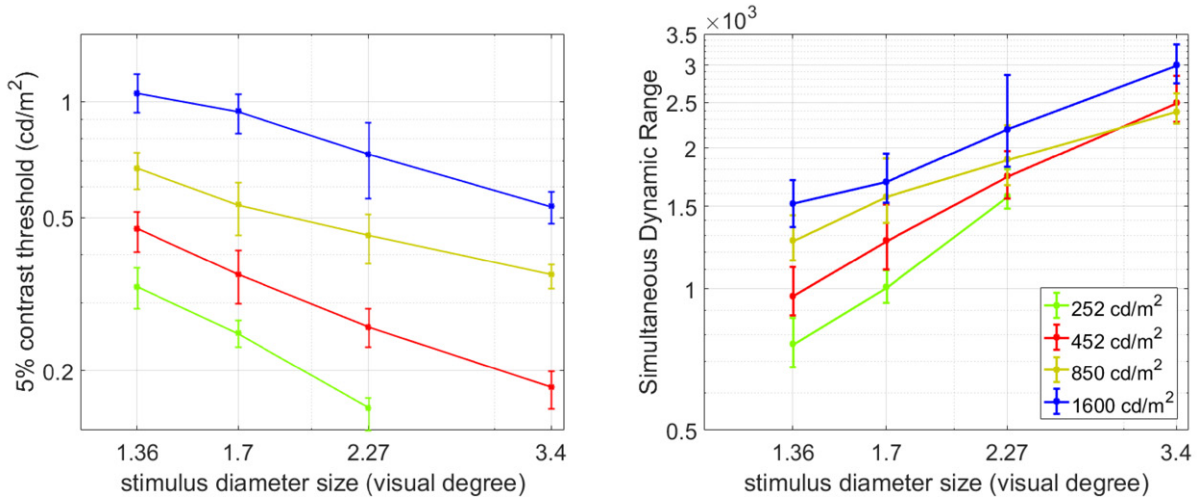

Figure 4. Summary result of OBS1 with repeat observations. The 5% contrast threshold is plotted on the left and the simultaneous dynamic range is plotted on the right. Error bars represent the 95% confidential interval through bootstrapping.

Clearly, for OBS1, the threshold showed a linear relationship against the log stimulus size for all four bright region luminance levels. The threshold decreases with increasing stimulus size for all four bright region settings. It is a reasonable result as the larger stimulus size would cause less glare in the visual system (on the commensurately larger dark regions) and more capability for local adaptation to the dark stimulus areas, hence lower thresholds. Moreover, the threshold increases monotonically with the increasing bright region settings. For the same stimulus size, the brighter the stimulus, the more glare it will cause in the visual system, hence impairing discriminating ability in the dark regions to a higher degree. Therefore, the threshold will increase with the increasing bright region luminance level.

The simultaneous dynamic range plot on the right showed the linear relationship against the stimulus size for all four bright region luminance levels. Moreover, in general, simultaneous dynamic range increases monotonically with the stimulus size for all four bright stimulus luminance levels. Furthermore, for the same stimulus size, the simultaneous dynamic range increases with the bright region luminance level mostly except for 3.4°. Another interesting finding is that for the smaller stimulus size, simultaneous dynamic range increases more significantly with the bright region luminance level than that of the larger stimulus size. For example, for 1.36° stimulus size, the simultaneous dynamic range of 850 cd/m^2 and 1600 cd/m^2 are both significantly higher than that of 452 cd/m^2 and 252 cd/m^2. The simultaneous dynamic range at 452 cd/m^2 is significantly higher than that of 252 cd/m^2 as well. While for 2.27° stimulus size, only the difference between 1600 cd/m^2 and 252 cd/m^2 is significant. For 3.4° stimulus size, there is no significant difference among the simultaneous dynamic ranges of all the three luminance levels of the bright regions. This indicates that the simultaneous dynamic range of the human visual system is gradually getting saturated with the increasing stimulus size, regardless of the luminance level of the bright stimulus.

Comparison between Result of OBS1 and Average Result. Figure 5 plots the comparison between the comprehensive result of the single observer OBS1 with the average result of five naive observers, which will be referred as average observer in the remainder of this paper. The error bar in the plots represent 95% confidence interval through bootstrapping. Bootstrapping is a series of binomial simulation, which generates a distribution of the estimated thresholds. The 95% confidence interval can be derived from the distribution. The data were plotted on log–log axes as well. For the measured threshold on the left of Fig. 5, the average observer also showed the threshold decreases monotonically with stimulus size for 452 cd/m^2, while not for 1600 cd/m^2. For 452 cd/m^2, the threshold of average observer decreases significantly at the three measured stimulus sizes, agreeing with the OBS1 data. For 1600 cd/m^2, the threshold of OBS1 showed monotonically decreasing relationship against stimulus size but insignificantly. The average observer did not demonstrate the decreasing against stimulus size for 1600 cd/m^2. Also, in general OBS1 showed lower threshold, i.e. higher sensitivity, than the average observer though insignificant for all conditions.

For the simultaneous dynamic range plot on the right in Fig. 5, the simultaneous dynamic range of the average observer increases with increasing stimulus size for 452 cd/m^2 but not for 1600 cd/m^2. Moreover, the simultaneous dynamic range with 1600 cd/m^2 bright stimulus is only significantly higher than that of 452 cd/m^2 for 1.7°. While for 2.27° and 3.4°, the simultaneous dynamic range of the average observer is almost the same for 452 cd/m^2 and 1600 cd/m^2. This, more significant difference for smaller stimulus size, agrees with that of OBS1. This showed a general trend that the impact of the bright stimulus luminance level over the simultaneous dynamic range becomes larger with the stimulus size decreasing.

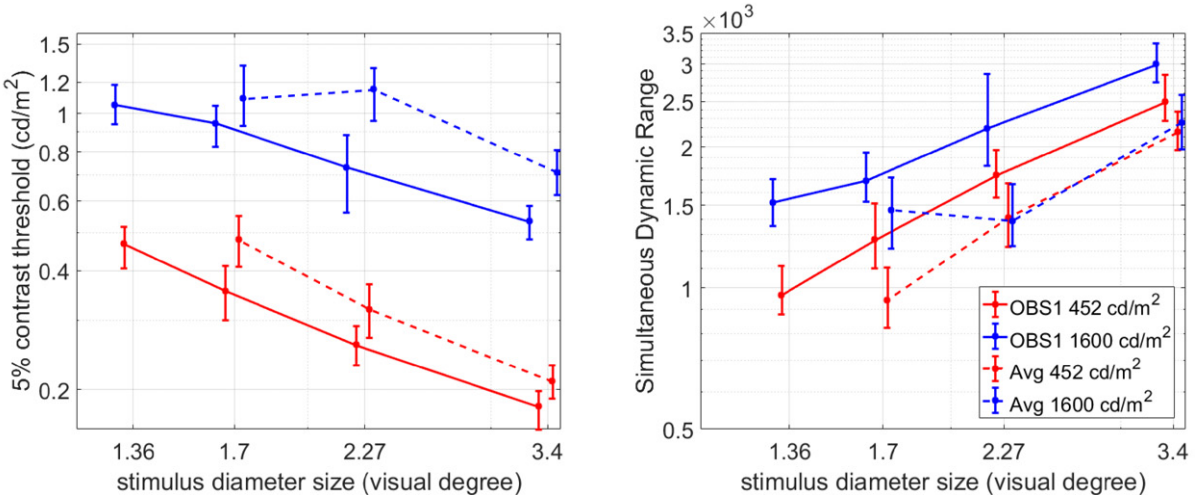

Figure 5. Comparison between result of OBS1 and the average result of five observers. The measured threshold of 5% contrast is plotted on the left, and the simultaneous dynamic range is plotted on the right. Both horizontal axes are the stimulus size. Line types represents OBS1 and average observer. Line color represents different luminance levels of the bright stimulus. Error bars represent 95% confidence interval.

3.2 *Experiment II*

3.2.1 *Experimental Images*

Experiment II focused on the effect of the spatial frequency of the Gabor pattern on simultaneous dynamic range. It is known that human visual system has the highest sensitivity at around 2–5 cpd for achromatic pattern, as a band pass function [15, 16]. According to the most recent study by Wuerger et al., the human visual system has highest sensitivity at 0.5–2 cpd for luminance level around 0.2–2 cd/m^2 [14]. The peak of the sensitivity is stable at around 2 cpd for luminance level between 20 and 7000 cd/m^2. Therefore, in this section the simultaneous dynamic range of four different spatial frequencies of the Gabor pattern were measured for one stimulus size as 2.27°, i.e. viewing distance as 3000 mm. The four different spatial frequencies were 1.2 cpd, 2 cpd, 4 cpd, and 8 cpd. The Gabor pattern, with fixed diameter as of 2.27°, making ≈2.7, 4, 8, 16 cycles for the four different frequencies. Two luminance levels for the bright regions were used, 452 cd/m^2 and 1600 cd/m^2.

3.2.2 *Procedure and Observers*

Experiment II followed the same as the flowchart in Fig. 3. The order of the experimental images was also randomized as well. Due to the COVID-19 pandemic, only one single observer, OBS1, participated in experiment II. OBS1 made 32 repetitions of all trials. Each measured threshold was derived from six to eight trials, called steps in the psychophysical method of constant stimuli.

3.2.3 *Result*

Figure 6 plots the result of experiment II, the impact of varying spatial frequency Gabor pattern. The horizontal axis is the spatial frequency of the Gabor pattern, and the vertical axis is the simultaneous dynamic range, $L_{\text{bright}}/L_{\text{threshold}}$. $L_{\text{threshold}}$ is measured threshold of the 5% contrast from the experiment. Both axes are in log scale. The error bars

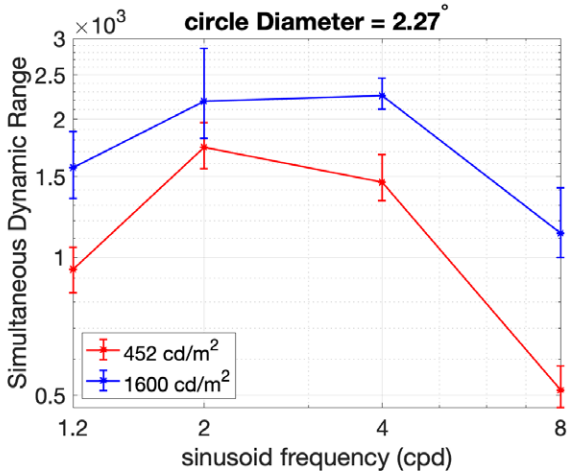

Figure 6. Result of experiment II for OBS1, the simultaneous dynamic range was plotted against the spatial frequency of the Gabor pattern for two bright region luminance level settings.

represent for the 95% confidence interval, derived through bootstrapping. Again, this is for stimulus size as 2.27°, i.e. viewing distance as 3000 mm.

Firstly, the result showed that the shape of simultaneous dynamic range as a function of spatial frequency is a band pass curve, similar to the traditional achromatic Contrast Sensitivity Function (CSF). Moreover, the peak simultaneous dynamic range appears around 2 cpd for 452 cd/m^2 and between 2 and 4 cpd for 1600 cd/m^2. This is slightly different from the recent study by Wuerger [14]. Wuerger reported the peak sensitivity 1–2 cpd for luminance level below 2 cd/m^2. Furthermore, there are two clear differences between the two bright luminance levels: (1) the simultaneous dynamic range is significantly higher of $L_{\text{bright}} = 1600$ cd/m^2 than that of $L_{\text{bright}} = 452$ cd/m^2, except at 2 cpd; (2) the bandwidth of the 1600 cd/m^2 curve is larger than that of 452 cd/m^2.

Overall, the experimental data showed similarity with a typical CSF curve, within the range of peak CSF, though demonstrating some difference from the most recent study on the low luminance level. Moreover, the spatial frequency dynamic range curve is clearly the bright region luminance level dependent. Overall, this result affirms the choice of stimulus spatial frequency in experiment I.

4. MODELING

The modeling goal was to derive a data-descriptive simultaneous dynamic range model as a function of the bright region luminance level and stimulus size in the investigated range. However, due to the limited data of the average observer, the model was derived based on the comprehensive data of the single observer, OBS1, from experiment I to generate a descriptive model form. The average observer data were then compared with the fitted model. Two different models were proposed to fit the experiment I data. One is linear model in log scale, which is clearly a fitting based on the experiment data. However, there is a fundamental drawback of the log linear model that there is no saturation level. Therefore, in the second model, a saturation level is included, a nonlinear model on the log scale. Both models have advantages and disadvantages. Since, there is no previous modeling, or similar experimental data on the direct simultaneous dynamic range measurement, no comparison with other studies can be made. Moreover, for experiment II, a log parabola function was used to model the simultaneous dynamic range as the function of the spatial frequency for each bright region luminance level. These models are only descriptive of the current psychophysical results and should not be taken as a general model of human visual perception without additional data collection and model validation.

4.1 *Experiment I Modeling*

Two different models were proposed to fit the simultaneous dynamic range as a function of stimulus size and the bright region luminance level. Both models were based on threshold prediction, which can be easily transformed into the simultaneous dynamic range. The first model is called log linear model, a linear function in log scale as in Eq. (3), where D stands for the diameter of the stimulus in the experimental image, DR means the simultaneous dynamic range. The constant parameters, k and a, of the linear function vary with the luminance level of the bright stimulus. The second model is a nonlinear function as in Eq. (4), where D is the diameter of the stimulus as well and k, n, a, b are constant parameters. These parameters will be derived for each bright stimulus luminance level.

$$\begin{aligned} \log_{10} L_{\text{threshold}} &= k \times log_{10} D + a \\ \log_{10} DR &= \log_{10} L_{\text{bright}} - \log_{10} L_{\text{threshold}} \end{aligned} \tag{3}$$

$$\begin{aligned} L_{\text{threshold}} &= k \times \left(1 - \frac{D^n}{D^n + b}\right) + a \\ \log_{10} DR &= \log_{10} L_{\text{bright}} - \log_{10} L_{\text{threshold}}. \end{aligned} \tag{4}$$

Table I. Optimized parameters for log linear and nonlinear fitting over experiment I data.

	Method 1 (log linear)		Method 2 (nonlinear)			
L_{bright}	k	a	k	n	b	a
252 cd/m^2	−1.419	−0.286	9.932	2.173	0.051	0.074
452 cd/m^2	−1.029	−0.204	9.823	1.647	0.065	0.096
850 cd/m^2	−0.676	−0.098	9.913	2.236	0.079	0.304
1600 cd/m^2	−0.761	0.135	9.282	0.708	0.179	−0.116

Figure 7 plots the original experiment data and best-fitting curves using the two methods. Each curve is best fitting for constant luminance level of the bright stimulus. The threshold fitting was plotted on the left and the simultaneous dynamic range was plotted on the right. The parameters of the two methods were listed in Table I. It can be found that, both methods fit the data well. In general, the nonlinear fitting method (dash line) works better than the log linear fitting method (solid line). The log linear fitting works best for 452 cd/m^2 and 1600 cd/m^2. The nonlinear method fits the mean threshold very well except for 252 cd/m^2. For the simultaneous dynamic range plot on the right, the nonlinear method showed advantage of including a saturation level with increasing stimulus size. The nonlinear fitting curves (dash line) showed clearly saturation around 3.4° for 252 cd/m^2, 452 cd/m^2 and 850 cd/m^2 but not for 1600 cd/m^2.

4.1.1 *Constrained fitting*

During the examination of the two methods, it was found that the three fitting lines (252 cd/m^2, 452 cd/m^2, and 850 cd/m^2) intersect with each other at almost the same position for the log linear method (recall solid lines on left in Fig. 7). Therefore, to simplify the log linear model, one constraint was added: the four fitting lines of the four L_{bright} will intersect at almost the same position. Moreover, for the nonlinear method 2 it was found that two of the four parameters in Eq. (4) can be set as constant across different L_{bright} while maintaining a good performance. The best performance was found for constant $b = 0.2$, $a = 0.1$. The optimized parameters of the two methods under the constrain are listed in Table II. The parameters, k and a, in method 1 can be simplified by a linear prediction. The number of the parameters in method 2 (Eq. (4)) can be reduced from 4 to 2.

Figure 8 plots the experimental data with the optimized constrained fittings. For method 1 (log-linear) fitting, the fitting lines change most for 252 cd/m^2 and 850 cd/m^2 with the constraint, but less change for 452 cd/m^2 and 1600 cd/m^2. While for the nonlinear method 2 fitting, the constraint does not change too much within the experimental stimulus size. For the nonlinear fitting method 2, the constant a stands for the saturation level, which is the threshold for very large stimulus size where the observers could adapt more to the dark stimulus in regardless of the bright region luminance

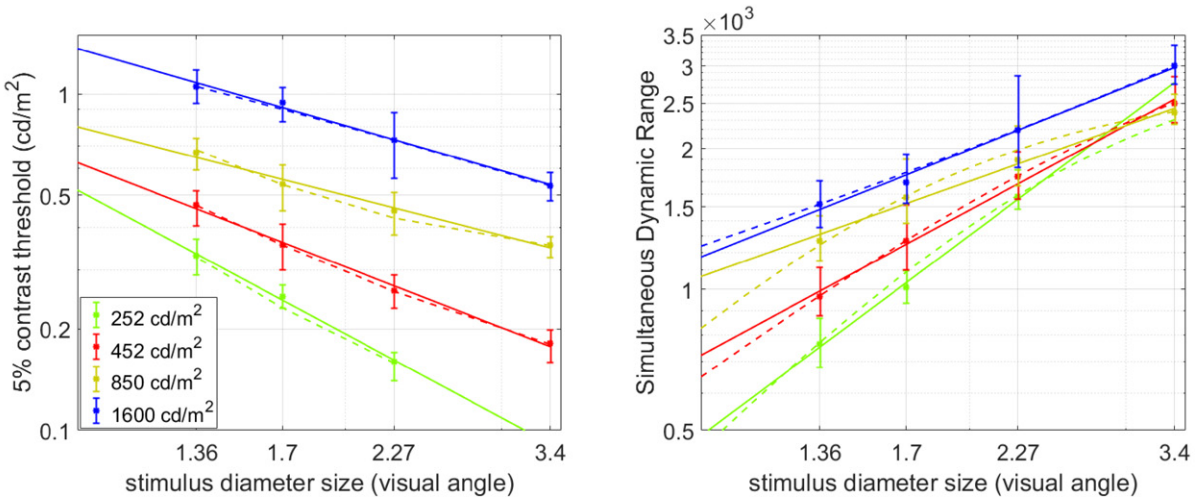

Figure 7. Result of experiment I for single OBS1 with method 1 (log-linear) in solid lines, and method 2 (nonlinear) in dash lines.

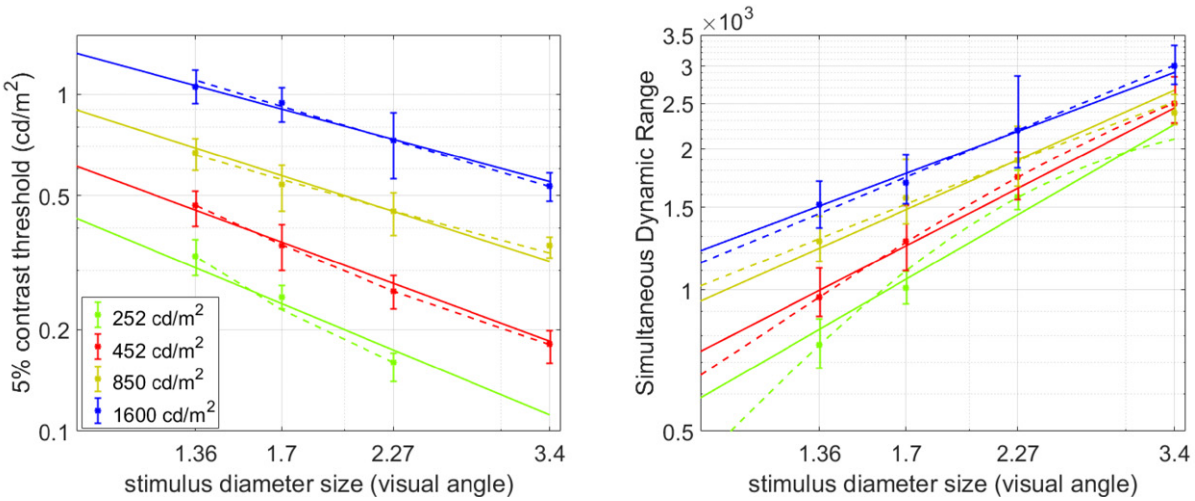

Figure 8. Result of experiment I for single OBS1 with constrained fitting. Method 1 fitting (log-linear) is in solid lines, and method 2 (nonlinear) is in dash line.

Table II. Optimized parameters under constrain for log linear and nonlinear fitting over experiment I data.

	Method 1 (log linear)		Method 2 (nonlinear)			
L_{bright}	k	a	k	n	b	a
252 cd/m^2	−1.0970	−0.3685	2.9032	2.7433	0.2	0.1
452 cd/m^2	−0.9761	−0.2140	3.5198	1.7505		
850 cd/m^2	−0.8454	−0.0469	4.3984	1.0231		
1600 cd/m^2	−0.7144	0.1204	7.8013	1.0035		

level. Therefore, the threshold would saturate for very large stimulus size. This is the advantage of the nonlinear fitting.

To compare the performance of the non-constrained optimization and the constrained optimization, the root-mean-square-error (RMSE) was computed for different L_{bright}. The RMSE in log unit, the same for the thresholds and the simultaneous dynamic ranges, are listed in Table III. Overall, the RMSE is below 0.03 in log unit (7% in linear scale), which is very small. With the constraint, the RMSE increases slightly. For 252 cd/m^2 and 850 cd/m^2 of method 1, the RMSE increases more under the constraint. The RMSE increases more only for 252 cd/m^2 of method 2. Overall, the RMSE increases slightly with the constraint but still small compared with the simultaneous dynamic range value, 3–3.3 log unit.

4.1.2 *Glare-based model*

As mentioned in the introduction, the glare caused by the bright stimulus is one of the main resource limiting the human visual system in discriminating the Gabor pattern. Therefore, the estimated glare over the dark stimulus is expected to be related with the 5% contrast pattern threshold. For glare estimation, there is a widely used Stiles-Holladay model as in Eq. (5), where β is the estimated glare, k, and n

Table III. RMSE in log unit, the same for $L_{threshold}$ and the simultaneous dynamic range, of the two methods, for no constraint and constrained conditions.

	RMSE (log_{10} unit)			
	Method 1 (log linear)		Method 2 (nonlinear)	
	No constraint	Constrained	No constraint	Constrained
252 cd/m^2	0.0077	0.0305	0.0172	0.0216
452 cd/m^2	0.0111	0.0132	0.0005	0.0013
850 cd/m^2	0.0116	0.0267	0.0114	0.0135
1600 cd/m^2	0.0097	0.0116	0.0104	0.0111

are constant, E is the illuminance from the source, and θ_G is the disparate visual angle between the glare source and the fixation. Stiles proposed $n = 1.5$ [17], and Holladay reported $n = 2$ [18]. McCann showed a program to compute the retinal contrast image considering the human visual system glare [19]. McCann's program is based on the CIE standard [20], which roughly adopts the $n = 2$ and $k = 10$.

$$\beta = k \times \frac{E}{(\theta_G)^n}. \tag{5}$$

Figure 9 plots the 5% contrast threshold against the mean of the estimated glare over the Gabor pattern area. This is a log–log plot. The error bars are the 95% confidence interval of OBS1 data. The solid lines are best fittings for the four bright stimulus luminance levels following Eq. (6), where k, and b are bright stimulus luminance dependent constants, β is the estimated glare. Surprisingly, the three lines of 252 cd/m^2, 452 cd/m^2 and 1600 cd/m^2 intersect at the same point. Therefore, constraining all the four fittings lines intersecting at the same point would reduce the parameters from 2 to 1 for each line as in Eq. (7), where k is luminance dependent, β_0 (3.43) and L_0 (0.051) are constants. The dashed lines in Fig. 9 are the optimized results under the constraint. All the constants and the RMSE are listed in Table IV. It can be found that, there is only slight change of the line of 850 cd/m^2, while the rest almost remain the same. Even under the constrain, all the fitting lines are within the 95% confidence intervals. The RMSE is very small in log unit, except for that of 850 cd/m^2 under the constrain (reaching 0.02 in log unit, 5% in linear unit).

$$\log_{10} L_{\text{threshold}} = k \times \log_{10} \beta + b \tag{6}$$

$$\log_{10} L_{\text{threshold}} = k \times (\log_{10} \beta - \log_{10} \beta_0) + \log_{10} L_0. \tag{7}$$

Clearly, the threshold has a positive linear relationship with the mean estimated glare for each bright region luminance level. Moreover, the slope of the fitting lines decreases with increasing bright region luminance level, which means the impact of the glare decreases with higher bright region luminance level. Also, for the same estimated glare level, the threshold is higher for the low luminance level of the bright region (smaller stimulus size) than that of the high luminance level (larger stimulus size).

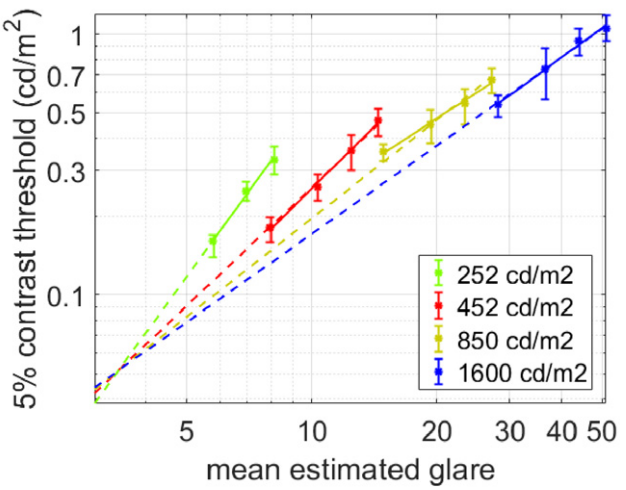

Figure 9. Mean results with 95% confidence interval error bars. The horizontal axis is the mean of the estimated glare over the Gabor pattern region. The vertical axis is the 5% contrast threshold. The solid lines are the best fittings for the four luminance levels. The dash lines are the optimized lines with constrain.

Table IV. Parameters for the glare-based model: bright stimulus luminance level dependent k and b Eq. (6), and k for Eq. (7).

	No constrain (Eq. (6))			Constrained (Eq. (7))	
	k	b	RMSE (log_{10})	k	RMSE (log_{10})
252 cd/m^2	2.168	−2.443	0.0097	2.189	0.0098
452 cd/m^2	1.579	−2.172	0.0102	1.509	0.0123
850 cd/m^2	1.036	−1.671	0.0107	1.254	0.0240
1600 cd/m^2	1.164	−1.952	0.0108	1.126	0.0114

4.2 *Experiment II Modeling*

Log parabola function has been used to model contrast sensitivity function (CSF) for a long time [16, 21–23]. Especially, the most recent work from Wuerger et al. showed that model works well for a high dynamic range from 0.02 cd/m^2 up to 7000 cd/m^2 [14]. Therefore, a log parabola was used to fit our experiment II data as well, as in Eq. (8). DR stands for the simultaneous dynamic range, $DR_{\max}$ is the maximum simultaneous dynamic range, f is the spatial frequency, $f_{\max}$ is the spatial frequency with the maximum simultaneous dynamic range, and b is the bandwidth.

$$\log_{10} DR = \log_{10} DR_{\max} - \left(\frac{\log_{10} f - \log_{10} f_{\max}}{b}\right)^2. \tag{8}$$

Figure 10 showed the log parabola fitting separately for 452 cd/m^2 and 1600 cd/m^2 in dash lines. Table V lists the optimized parameters for 452 cd/m^2 and 1600 cd/m^2. $DR_{\max}$ is higher of 1600 cd/m^2 than that of 452 cd/m^2. Moreover, the bandwidth b of 1600 cd/m^2 is larger than that of 452 cd/m^2. Interestingly, $f_{\max}$ is very close for 452 cd/m^2 and 1600 cd/m^2. Overall, the fitting simultaneous of 1600 cd/m^2 is higher than that of 452 cd/m^2 in the range between 1.2 cpd and 8 cpd. Obviously, in this experiment data, the $f_{\max}$ is

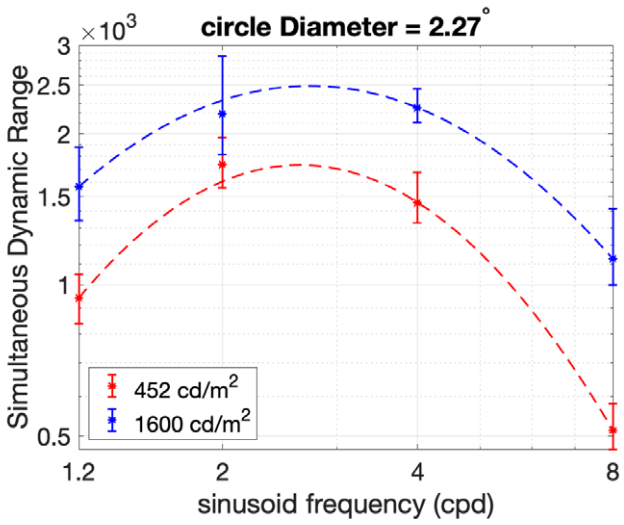

Figure 10. Best log parabola fitting for 452 cd/m^2 and 1600 cd/m^2 separately for varying spatial frequency patterns.

Table V. Optimized parameters for log parabola fitting over experiment II data.

L_{bright}	$\log_{10} DR_{max}$	f_{max}	b	RMSE ($\log_{10}$ unit)
452 cd/m^2	3.24	2.6	4.6	0.0170
1600 cd/m^2	3.40	2.7	6.2	0.0135

larger than the f_{max} from Wuerger's work [14], 0.5–2 cpd. Moreover, the RMSE in $\log_{10}$ unit listed in Table V showed only 0.017 and 0.0135 of the log parabola fitting.

5. DISCUSSION

5.1 *Experiment I*

Simultaneous dynamic range is an important concept describing human visual system's capability in discriminating the details when high dynamic range stimuli were presented at the same time. This value has been measured a few times in previous studies, range from 2 to 4 log units. However, none of them measured the simultaneous dynamic range in a direct way through psychophysical methodology. The most recent studies from Kunkel et al. reported a value of 3.7 log units simultaneous dynamic range through measuring the threshold of a Gabor pattern with a certain contrast level above and below the adapting level separately [9]. This indirect measurement method would overestimate the actual simultaneous dynamic range due to the lack of stable adaptation and lack of glare consideration. This could explain why the reported value from Kunkel is higher than most previous studies, as well as this study. So far, there is no other direct measurement of the simultaneous dynamic range in the perspective of the observers. No further comparisons with any other studies can be made.

In this study, a comprehensive direct measurement of the simultaneous dynamic range was used to propose a model in predicting the simultaneous dynamic range of 5% contrast in dark stimulus as a function of the stimulus size. Two different methods were proposed as log-linear and nonlinear model. The parameters of both are bright-stimulus luminance level dependent. The log-linear model has its advantage of simplicity. However, it does not include the saturation feature, which theoretically should be included in a comprehensive model for extreme large stimulus size. However, both models are based on one single observer's data. Therefore, it is necessary to examine the model with the limited collected average observer's data. Figure 11 plots the examination of the average observer's data of the two bright-region luminance levels, 452 cd/m^2 and 1600 cd/m^2 with two constrained fitting models. Table VI lists the RMSE of the two fitting methods over the two luminance levels. In general, the RMSE is very small in $\log_{10}$ unit, no more than 0.047 compared with 3.3 log unit simultaneous dynamic range. Moreover, the two methods showed the same performance for 1600 cd/m^2 luminance level in terms of RMSE, higher than that of 452 cd/m^2. For 452 cd/m^2, method 2 showed almost a perfect fitting, while the RMSE is higher for method 1 fitting. Though the RMSE of the average observer's fitting is higher than the OBS1's data in Table III, the examination of the model using average observer's data promises the generalization of the simultaneous dynamic range model for the 5% contrast, as a function of the stimulus size. The generalization of the model would require more observers' experimental data.

Table VI. RMSE in log unit, the same for $L_{threshold}$ and the simultaneous dynamic range, of the two methods with constrain for average observer's data.

	RMSE ($\log_{10}$ unit)	
	Method 1 (log linear)	Method 2 (nonlinear)
452 cd/m^2	0.034	0.005
1600 cd/m^2	0.047	0.047

Glare-based model presented in the modeling works well with OBS1 data. It showed that for the same estimated glare the threshold for higher luminance level (larger stimulus size) is lower than that of the lower luminance level (smaller stimulus size). There are two possible explanations: (1) the pupil size will change with the bright stimulus luminance level and the stimulus size. While the glare model does not take that into consideration. (2) The glare itself is not enough to explain the 5% contrast threshold in this pattern. Moreover, there is a difference between the glare and threshold. Choi and Alabni et al., proposed an image-dependent model, where the threshold was predicted with accumulated glare from the rest of the image [24]. Choi reported a background-dependent n for a certain region of interest (ROI). Though with only two discrete backgrounds, the result showed an interesting point that n should vary with background, maybe even with specific pattern. Because the background and the image content would affect the state of the adaptation, maybe the pupil size as well. Though, lacking of such research work prevents a further analysis of the glare-based model, Choi's work

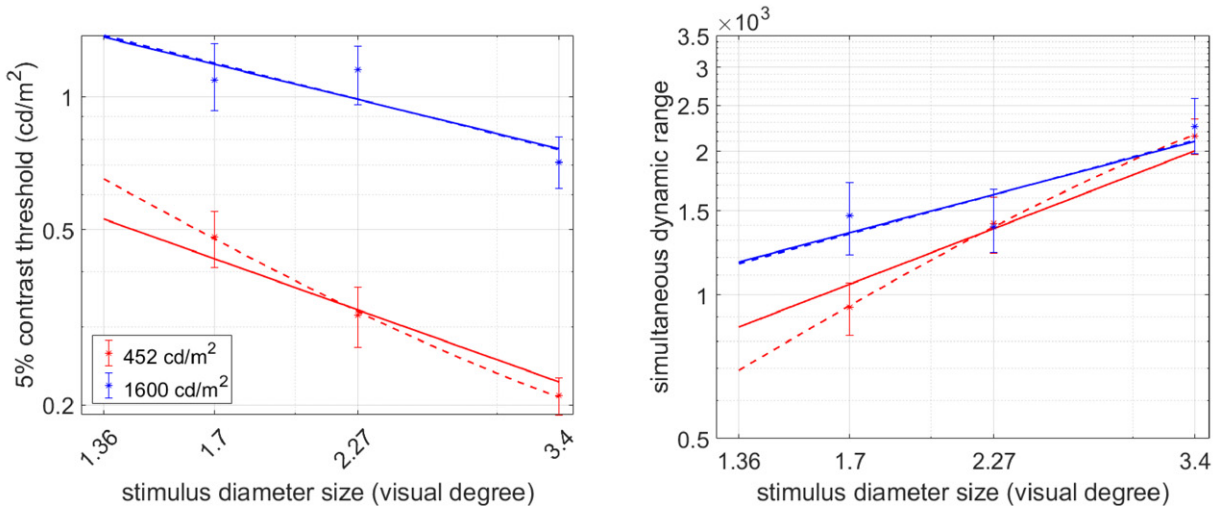

Figure 11. Best log-linear and nonlinear fittings for 452 cd/m^2 and 1600 cd/m^2 separately of the naive observers' data.

Table VII. RMSE in log unit, the same for $L_{threshold}$ and the simultaneous dynamic range, of the fitting results for average observer's data against the estimated glare (in Fig. 12).

	RMSE (log_{10} unit)	
	No constrain	Constrained
452 cd/m^2	0.0128	0.0163
1600 cd/m^2	0.0471	0.0509

here showed the validation of using glare to predict the 5% contrast pattern (the simultaneous dynamic range) for the given bright region luminance level and the threshold prediction is background/image content dependent. The bright stimulus dependent glare-based model is consistent with Choi's work.

This glare-based model will be tested with the observers' data as well as the other two models. The observers' data are fitted with Eq. (6), and Eq. (7). Figure 12 plots the results and Table VII lists the RMSE as the fitting error. The line fits the data of 452 cd/m^2 luminance level very well, much better than that of 1600 cd/m^2. Clearly, the constrain does not change the fitting line too much. The RMSE is slightly higher for the constrained fitting, reaching 0.0509 log unit (12% in linear scale) for 1600 cd/m^2. Clearly, the error is higher for 1600 cd/m^2, but still it is within the 95% confidence interval. Again, the lack of more observers' data prevents the generalized model but the fitting of average observer's data showed the promising performance of the model.

Vangorp, Myszkowski et al. proposed a model of local adaptation, predicting threshold over a certain luminance level under a background adapting level [25]. The model contains a visual system Point-Spread-Function, similar to a glare model, an inverse contrast sensitivity function, a maladaptation, and an optimized local adaptation. The local adaptation model was optimized based on a series

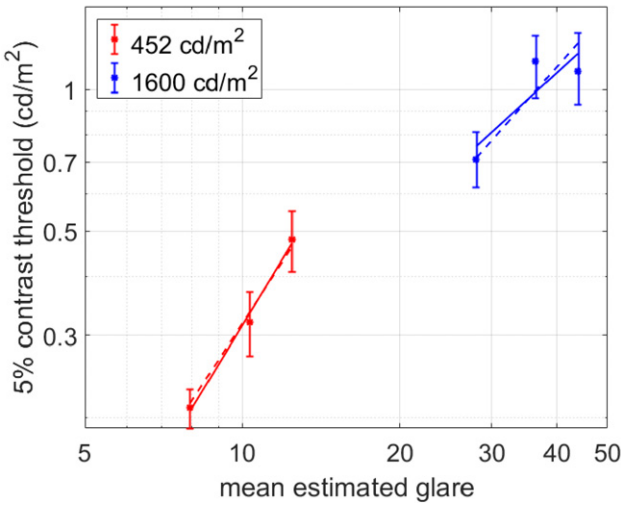

Figure 12. Best log-linear fittings without constrain (solid lines) and with constrain (dash lines) for 452 cd/m^2 and 1600 cd/m^2 separately of the naive observers' data.

of experimental data. One key was measuring the thresholds over different base luminance level under different background adapting levels. However, there was only very limited data about 0.5 cd/m^2 target over very bright background/adapting levels. Moreover, the target was only 0.2° with a sharp edge. The model was focusing more over predicting the adaptation over a luminance level clearly above our measured threshold. In this study, the goal to was determine the threshold where human can see a certain contrast details. Vangorp clearly made some predictions about the visible dynamic range, using a SNR as 4:1 criteria, which is not perceptual meaningful. Moreover, the predicted visible dynamic range was computed for an entire scene across images. So, the result is image-dependent. Therefore, the model is more suitable for an natural scenes while our study is a fundamental study of visual simultaneous dynamic range. Additionally, the model did not show the

impact of different viewing distances, which is a key in this study. Lastly, the model itself is very complex with optimization parameters over several other aspects, such as orientation, contrast mask. Considering the fundamental difference between the model and this study, no comparison was made with Vangorp's model.

Moreover, this study, focusing on simultaneous dynamic range and the dependencies of simultaneous dynamic range, should be separated from the research about the sensitivity to perfect black. Mantiuk, Daly, et al. presented work about the minimal requirement of black level over different surrounding images [26]. Their work explored the level where human observers cannot tell the difference between the threshold and 0 luminance. There is no requirement about seeing contrast in the dark region. This threshold to 0 cd/m^2 was further explored and modeled by Jiang, Bodner et al. [27].

5.2 *Experiment II*

Impact of Gabor pattern spatial frequency was explored and modeled in experiment II. The log parabola function fits the experimental result well, though the log parabola was used for traditional CSF model mostly. Experiment II is slightly different from the traditional CSF measurement, where the sensitivity was measured for varying spatial frequencies at a certain mean luminance level. The threshold of a constant relative contrast level, 5%, was measured for different spatial frequencies of the bright dark alternating pattern. Another critical difference is the adapting time. For luminance level between 0.4 and 2 cd/m^2 Gabor pattern, it usually requires much longer adaptation time, for example observers spent 5–10 min to adapt to the luminance level for 0.02 cd/m^2 and 0.2 cd/m^2 in Wuerger's experiment I [14]. However, the bright dark spatially-alternating pattern would prevent the complete adaptation to dark stimulus. The observer did not spend time longer than 10 s. Moreover, the Gabor pattern has large enough size to ensure enough cycles of the high spatial frequency, e.g. 16 cycles for 8 cpd. This meets the minimum of 7 cycles from Barak's study [28]. Though Manituk also reported the target size impact over CSF at low luminance level [29], the target size is smaller than that in this study. Manituk's work can not be compared with our data directly. However, the data from Manituk's work, Figure 8, showed the impact of increasing size (up to 1.5°) decreases. Therefore, for the target size 2.27° in this experiment, we can speculate the very little impact due to the limited target size. Experiment II is representative for the spatial frequency effect on the simultaneous dynamic range.

In this study, the peak simultaneous dynamic range was found around 2.6/2.7 cpd, which is within the range of the traditional peak CSF 2–5 cpd [15, 30]. However, this is slightly higher than the recent study of the low luminance level from Wuerger, where the peak was found no more than 2 cpd [14]. Two facts may contribute to the difference: the low cycles (2 full cycles) in Wuerger's data, and the observers in Wuerger's experiment adapted more complete to that low luminance level with the traditional CSF measurement. The peak simultaneous dynamic range around 2.6–2.7 is a reasonable result, not conflicting with previous reported data.

6. CONCLUSION

In this study, the simultaneous dynamic range was measured directly through the bright dark spatially-alternating pattern for different stimulus sizes with varying bright region luminance level. The simultaneous dynamic range was found to be bright area luminance-level dependent, even for a constant 5% contrast Gabor pattern. Within 1600 cd/m^2 bright-region luminance level, the simultaneous dynamic range was found to increase monotonically with the bright-area luminance level but gradually saturated. Moreover, the simultaneous dynamic rang was found to increase with the stimulus size. A maximum value of 3.3 log units for average observer, 3.47 for OBS1, was found for 1600 cd/m^2 bright-area luminance level of 3.4° stimulus size. Two different methods were proposed to fit the experimental data. Both methods work well for the experiment I data. The method 1, log linear, has an advantage of simplicity but not including a saturation level for extreme large size. Method 2, a nonlinear method, fits the data better in terms of RMSE. Moreover, method 2 has advantage of including the saturation level for increasing size but requiring nonlinear parameters interpolation. Fitting average observer's data with the two methods showed the promising future of generalizing the model for observers' data. Very similar conclusion can be found for the glare-based model, which fits the 5% contrast threshold against the estimated glare for a given bright stimulus luminance level. It can be found that the linear fitting works well but the slope and offset of the line are bright stimulus luminance level dependent. It works well for the average observer's data. All these demonstrated that the simultaneous dynamic range can be predicted with a simple model with bright region luminance level dependent parameters. However, lack of average observer's data prevents a further generalization of the model. Experiment II showed the impact of spatial frequency of the Gabor pattern on the simultaneous dynamic range. The log parabola function, a band pass curve, models the impact well, similar to the achromatic CSF model. The peak simultaneous dynamic rang appeared around 2.6 cpd for both luminance levels. This is within the range of the traditional peak CSF range (2–5 cpd). The presented model is based on one single observer data. The future step of the spatial frequency effect would be generalizing the model with a comprehensive observers' data.

All proposed models are based on OBS1 data with a promising demonstration of some average observer's data. The work should not be considered a general model at this point. Therefore, the major future work would be collecting more observers' data to generalize the simultaneous model. Also, in addition to the 5% contrast level, more contrast levels can be explored for a comprehensive simultaneous dynamic range model.

REFERENCES

[1] H. Seetzen, L. A. Whitehead, and G. Ward, "54.2: a high dynamic range display using low and high resolution modulators," *SID Symposium Digest of Technical Papers* (Wiley Online Library, Hoboken, NJ, 2003), Vol. 34, pp. 1450–1453.

[2] H. Seetzen, W. Heidrich, W. Stuerzlinger, G. Ward, L. Whitehead, M. Trentacoste, A. Ghosh, and A. Vorozcovs, "High dynamic range display systems," *ACM SIGGRAPH 2004 Papers* (Association for Computing Machinery, New York, NY, 2004), pp. 760–768.

[3] S. Daly, T. Kunkel, X. Sun, S. Farrell, and P. Crum, "41.1: distinguished paper: viewer preferences for shadow, diffuse, specular, and emissive luminance limits of high dynamic range displays," *SID Symposium Digest of Technical Papers* (Wiley Online Library, Hoboken, NJ, 2013), Vol. 44, pp. 563–566.

[4] A. G. Rempel, W. Heidrich, H. Li, and R. Mantiuk, "Video viewing preferences for HDR displays under varying ambient illumination," *Proc. 6th Symposium on Applied Perception in Graphics and Visualization* (ACM, New York, NY, 2009), pp. 45–52.

[5] J. A. Ferwerda, S. N. Pattanaik, P. Shirley, and D. P. Greenberg, "A model of visual adaptation for realistic image synthesis," *Proc. 23rd Annual Conf. on Computer Graphics and Interactive Techniques* (ACM, New York, NY, 1996), pp. 249–258.

[6] R. L. Myers, *Display Interfaces: Fundamentals and Standards* (John Wiley & Sons, Hoboken, NJ, 2003).

[7] D. Purves and R. B. Lotto, *Why We See What We Do: An Empirical Theory of Vision* (Sinauer Associates, Sunderland, MA, 2003).

[8] R. A. Normann and I. Perlman, "The effects of background illumination on the photoresponses of red and green cones," J. Physiol. **286**, 491–507 (1979).

[9] T. Kunkel and E. Reinhard, "A reassessment of the simultaneous dynamic range of the human visual system," *Proc. 7th Symposium on Applied Perception in Graphics and Visualization* (ACM, New York, NY, 2010), pp. 17–24.

[10] P. G. Barten, "Formula for the contrast sensitivity of the human eye," Proc. SPIE **5294**, 231–238 (2003).

[11] "Apple pro XDR display white paper," https://www.apple.com/pro-display-xdr/pdf/Pro_Display_White_Paper_Feb_2020. Accessed: 2020-05-30.

[12] "CR100 tristimulus colorimeter," https://www.colorimetryresearch.com/products/cr-100. Accessed: 2020-04-30.

[13] P. G. Engeldrum, *Psychometric Scaling: A Toolkit for Imaging Systems Development* (Imcotek Press, Winchester, MA, 2000).

[14] S. Wuerger, M. Ashraf, M. Kim, J. Martinovic, M. Pérez-Ortiz, and R. K. Mantiuk, "Spatio-chromatic contrast sensitivity under mesopic and photopic light levels," J. Vis. **20**, 23 (2020).

[15] D. Kelly, "Visual contrast sensitivity," Optica Acta: Int. J. Opt. **24**, 107–129 (1977).

[16] A. B. Watson and A. J. Ahumada, "A standard model for foveal detection of spatial contrast," J. Vis. **5**, 6–6 (2005).

[17] W. S. Stiles, "The scattering theory of the effect of glare on the brightness difference threshold," Proc. R. Soc. Lond. B, Containing Papers of a Biological Character**105**, 131–146 (1929).

[18] L. Holladay, "The fundamentals of glare and visibility," J. Opt. Soc. Am. **12**, 271–319 (1926).

[19] J. J. McCann and V. Vonikakis, "Calculating retinal contrast from scene content: a program," Frontiers Psychol. **8**, 2079 (2018).

[20] J. Vos, B. Cole, H. Bodmann, E. Colombo, T. Takeuchi, and T. Van Den Berg,"CIE equations for disability glare," *CIE TC Report CIE* **146**, 27 (2002).

[21] A. J. Ahumada Jr and H. A. Peterson, "Luminance-model-based DCT quantization for color image compression," Proc. SPIE **1666**, 365–374 (1992).

[22] A. M. Rohaly and C. Owsley, "Modeling the contrast-sensitivity functions of older adults," J. Opt. Soc. Am. A **10**, 1591–1599 (1993).

[23] Y. J. Kim, A. Reynaud, R. F. Hess, and K. T. Mullen, "A normative data set for the clinical assessment of achromatic and chromatic contrast sensitivity using a qCSF approach," Investigative Ophthalmol. Visual Sci. **58**, 3628–3636 (2017).

[24] M. Choi, L. Albani, and A. Badano, "An image-dependent model of veiling glare effects on detection performance in large-luminance-range displays," Proc. SPIE **8318**, 831804 (2012).

[25] P. Vangorp, K. Myszkowski, E. W. Graf, and R. K. Mantiuk, "A model of local adaptation," ACM Trans. Graph. (TOG) **34**, 1–13 (2015).

[26] R. Mantiuk, S. Daly, and L. Kerofsky, "The luminance of pure black: exploring the effect of surround in the context of electronic displays," Proc. SPIE **7527**, 75270 (2010).

[27] F. Jiang, B. Bodner, S. P. Farnand, and M. J. Murdoch, "34-3: visual sensitivity to 'perfect' black," *SID Symposium Digest of Technical Papers* (Wiley Online Library, Hoboken, NJ, 2021), Vol. 52, pp. 458–461.

[28] R. Barakat and S. Lerman, "Diffraction mages of truncated, one-dimensional, periodic targets," Appl. Opt. **6**, 545–548 (1967).

[29] R. Mantiuk, K. J. Kim, A. G. Rempel, and W. Heidrich, "HDR-VDP-2: a calibrated visual metric for visibility and quality predictions in all luminance conditions," ACM Trans. Graph. (TOG) **30**, 1–14 (2011).

[30] F. L. Van Nes and M. A. Bouman, "Spatial modulation transfer in the human eye," J. Opt. Soc. Am. **57**, 401–406 (1967).